Front. Phys. China, 2008, 3(1): 105－111
DOI 10.1007/s11467-008-0012-4

REVIEW ARTICLE

Kong-qing YANG, Lei YANG, Bai-hua GONG, Zhong-cai LIN, Hong-sheng HE, Liang HUANG

Geographical networks: geographical effects on network properties

Abstract Complex networks describe a wide range of systems in nature and society. Since most real systems exist in certain physical space and the distance between the nodes has influence on the connections, it is helpful to study geographical complex networks and to investigate how the geographical constrains on the connections affect the network properties. In this paper, we briefly review our recent progress on geographical complex networks with respect of statistics, modelling, robustness, and synchronizability. It has been shown that the geographical constrains tend to make the network less robust and less synchronizable. Synchronization on random networks and clustered networks is also studied.

Keywords complex networks, network properties, geographical networks, synchronization, clustered networks

PACS numbers 05.45.Xt, 87.10.+e, 87.18.Bb, 89.75.Hc

Complex networks provide powerful tools to investigate complex systems in nature and society [1–3]. The properties of complex systems are affected by the geographical distribution of the components. For example, routers of the Internet [4] and transport networks [5, 6] lay on the two-dimensional surface of the globe; world-wide airport network is confined by the geography [7–9]; neuronal networks in brains [10] occupy three-dimensional space. Thus it is helpful to study the geographical complex networks [11–19].

To be specific, for the Chinese railway system, viewing the stations as "nodes" and rails as "links", the railway system is actually a complex geographical network. Our recent statistics on 3431 stations and 2147 trains nationwide [20] reveals that for this network, the clustering coefficient is almost zero, indicating sparse connections between the stations, therefore it is a tree network. This is the most economic way to construct a transportation network. On the other hand, viewing the stations as "nodes" and say if there is a link between two stations if at least one train stops at both stations, the railway system can be viewed as a geographical traffic network. Statistics reveals that this traffic network has large clustering coefficients ($\langle C\rangle = 0.83$) and small average network distance ($\langle d\rangle = 3.27$), that is, starting from any station, one only need to transfer at most twice to reach another station (could be a very small station) through the railway system. The degree distribution is scale-free. Consequently, the railway traffic network is a small world network with scale-free property.

To investigate the effect of geographical constrains on network properties, we first proposed a geographical network model with a tunable parameter to control the geographical effects [21], then studied the percolation problem [22, 23], cascading breakdown [24], and synchronization [25] on this network model to find out how the geographical constrains affect these network properties. Synchronization on random networks [26] and on clustered networks [27] is also discussed.

In this paper, we mainly focus on scale-free (SF) networks, i.e., the degrees of nodes satisfy a power law distribution: $P(k) \sim k^{-\lambda}$, for their ubiquity in real systems [1–3]. The network is generated as follows [21]. It begins with an $L\times L$ lattice, with periodical boundary conditions, and for each

Kong-qing YANG[1,2] (✉), Lei YANG[3,2], Bai-hua GONG[2], Zhong-cai LIN[1], Hong-sheng HE[1], Liang HUANG[4]

[1] Center for Complex Systems, Jimei University, Xiamen 361021, China
[2] Department of Physics, Lanzhou University, Lanzhou 730000, China
[3] Institute of Modern Physics, Chinese Academy of Science, Lanzhou 730000, China
[4] Department of Electrical Engineering, Arizona State University, Tempe, Arizona 85287, USA
E-mail: yangkq@jmu.edu.cn

Received October 20, 2007; accepted November 8, 2007

node assigned a degree k drawn from the prescribed SF degree distribution $P(k) \sim k^{-\lambda}$, $k \geqslant m$. Then a node i is picked out randomly; according to a Gaussian weight function $f_i(r) = D\mathrm{e}^{-(r/A\sqrt{k_i})^2}$, it selects other nodes and establishes connections until its degree quota k_i is filled or until it has tried many enough times. Duplicate connections are avoided. The process is carried out for all the nodes in the lattice. The clustering parameter A controls the average spatial distance of the connections, therefore controls the geographical constrains on the network topologies. For large A limit, e.g. $A\sqrt{m} \gg L$, the weight function will be trivial, and the network becomes a SF random (SFR) network, i.e., random in network connections. For small A, the network approaches lattice embedded SF (LESF) networks with nearest neighbor connections [12, 13]. Here, we assume that the time scales governing the dynamics are much smaller than that characterizing the network evolvement. Thus, the static geographical network models are suitable for discussing the problem under investigation. Figure 1 shows the direct chemical shell structure [12, 13], with different gray levels depicting different shells consisting of nodes with the same network distance from a given node, which is assumed to be the central node in each graph. Along with WLESF, the LESF model and the Scale-Free Random model (SFR) are also presented. Here, λ is fixed to 3.0 for all the three models, and A is varied as $1, 2, 3,$ and 5 in WLESF. As A goes larger, the shell boundary blurs and finally disappears as that of random graphs. The shell graph of WLESF shows an obvious structural transition from the LESF model to the SFR model.

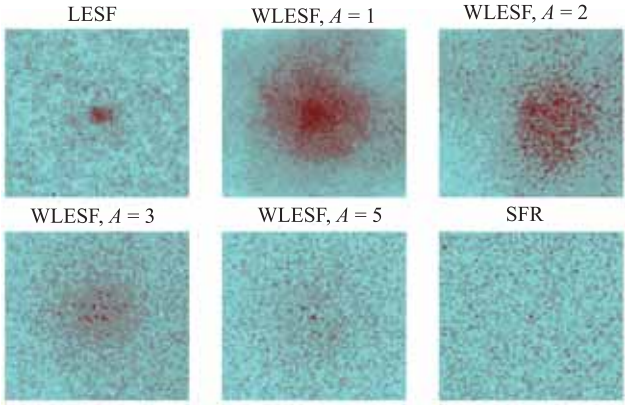

Fig. 1 Chemical shells of WLESF model, together with that of LESF model and SFR model. Each shell graph has a size of 195×195.

When losing nodes of fraction p, the remaining nodes of a network may still have a spanning cluster that most of the nodes are on this cluster and there are paths from one node to another globally. However, when losing enough nodes, at a certain point (percolating threshold p_c), the spanning cluster breaks into small pieces, and no path exist for global information transmission, that is, *the network breakdowns*. The heterogeneity of the degrees often makes the scale-free networks sensitive to intentional attacks (nodes with largest degrees are removed from the network first) [28−30], while it is resilience to random breakdowns (node are removed with the same probability p) [30, 31]. Figure 2 shows the dependence of p_c on A for both intentional attack and random removals. As A increases, p_c becomes larger, means it needs to remove more nodes to break the spanning clusters. Therefore, as the network is more loosely connected (average spatial distance is larger), the network is more robust to losing nodes.

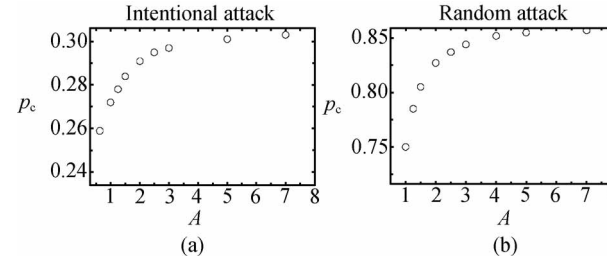

Fig. 2 Percolation transition point p_c versus cutoff parameter A. The upper and lower boundaries indicate the values of p_c of SFR and LESF model respectively. **(a)** is for intentional attacks and **(b)** is for random attacks. For each data, $N = 10000$, $\lambda = 3.0$ and $\langle k \rangle = 8$.

To better understand the numerical results, we employ the generating function method to determine the percolation threshold for networks with different clustering properties. Here the clustering properties can be simply depicted by the clustering coefficient, which counts for the triangles (3-cycles) in the network, and it can also be represented by the number of rectangles (4-cycles), and generally by the number of L-cycles. In the following, a general relation of the percolation threshold $q_c = 1 - p_c$ and the number of L-cycles for a random network with arbitrary degree distribution is determined. As an example, the dependence of q_c on the clustering coefficient is obtained.

For uniform occupations (or random failures), the percolation threshold of random tree-like networks is $q_c = \langle k \rangle / \langle k(k-1) \rangle$ [31, 32]. It could be obtained by the condition that the average cluster size diverges, or equivalently, the average size of clusters that reached by following an edge diverges. A real network is usually clustered and contains certain amount of cycles. If the number of cycles is small, (e.g. each node belongs to at most one cycle) the generating function process can be extended to cope with the random percolation problem. In a recent paper [23], after lengthy deviation, we finally get the percolation threshold q_c:

$$q_{\rm c}=\frac{\langle k\rangle}{\langle k(k-1)\rangle-2\langle kn_L(k)\rangle\left[1-\dfrac{2-q_{\rm c}^{l_1}-q_{\rm c}^{l_2}}{2(1-q_{\rm c})}\dfrac{q_{\rm c}\langle k(k-2)\rangle}{\langle k\rangle}\right]} \quad (1)$$

When $n_L = 0$, this result degenerates to the known result of the tree-like networks: $q_{\rm c} = \langle k\rangle/\langle k(k-1)\rangle$. In general $q_{\rm c} < 1$, as $L \to \infty$, $q_{\rm c}^{l_1}$ and $q_{\rm c}^{l_2}$ limit to 0, Eq. (1) reduces to a second order equation for $q_{\rm c}$. The root with physical meanings is $q_{\rm c} = \langle k\rangle/\langle k(k-1)\rangle$, which is just the percolation threshold of the tree-like networks. This means that the cycles of infinite length do not affect the percolation thresholds. The numerical tests for several typical data values show that, for the same number of cycles, $q_{\rm c}$ is an increasing function of $q_{\rm c}^{l_1} + q_{\rm c}^{l_2}$. The higher the cycle order L is, the less influence it will be. Thus the most influential cycles are 3-cycles, which could be expressed by the clustering coefficients.

For $L = 3$, $l_1 = l_2 = 1$. If the clustering coefficient $C = \langle C(k)\rangle$ is small enough, we may assume that two triangles could only have at most one common node. A node with degree k reached by an edge will belong to on average $n_3(k) = (C(k)(k-1)(k-2) + C(k)(k-1))/2 = C(k)(k-1)^2/2$ triangles. Eq. (1) will reduce to

$$q_{\rm c}=\frac{\langle k\rangle}{\langle k(k-1)\rangle-\left(1-q_{\rm c}\dfrac{\langle k(k-2)\rangle}{\langle k\rangle}\right)\langle C(k)k(k-1)^2\rangle} \quad (2)$$

The percolation threshold $q_{\rm c}$ increases monotonically with $\langle C(k)k(k-1)^2\rangle$. It is straightforward that when $C(k)$ limits to 0, $n_3 \to 0$, $q_{\rm c}$ returns to $\langle k\rangle/\langle k(k-1)\rangle$. On the other hand, if $\langle C(k)k(k-1)^2\rangle$ diverges, $q_{\rm c}$ maximizes to $\langle k\rangle/\langle k(k-2)\rangle$.

Although Eq. (2) holds only for the case of small clustering coefficient C, the analysis above indicates that for large C, or if the network has higher order cycles, the fraction of edges that inter-connect existed nodes in a local cluster will further increase. Thus the number of efficient edges connecting to "new" nodes (in comparison to the nodes within the local cluster) may be even smaller, which results in a higher percolation threshold. Thus when a network is more clustered, or has more cycles—not only of order 3—it will be less robust.

Figure 3 shows the clustering coefficients for different A values. For each given degree exponent λ, the larger the A is, the looser the local cluster is, as a result, the smaller the clustering coefficient is. This is consistent with the result that networks with larger A is more robust to percolation.

In many realistic situations the flow of physical quantities in the network, as characterized by the loads on nodes, is important. For such networks where loads can redistribute among the nodes, a failure of a node can lead to a cascade of overload failures, which can in turn cause the entire or a substantial part of the network to collapse. Many real systems-e.g., power grid networks, traffic lines, Internet-are sensitive to cascading failures and are located on the two-dimensional global surface, the influence of geographical structures on cascading breakdowns is thus of high importance. Here, by studying the influence on the cascading behavior of the networks by varying A, we uncovered how the geographical structures affect cascading breakdowns [24].

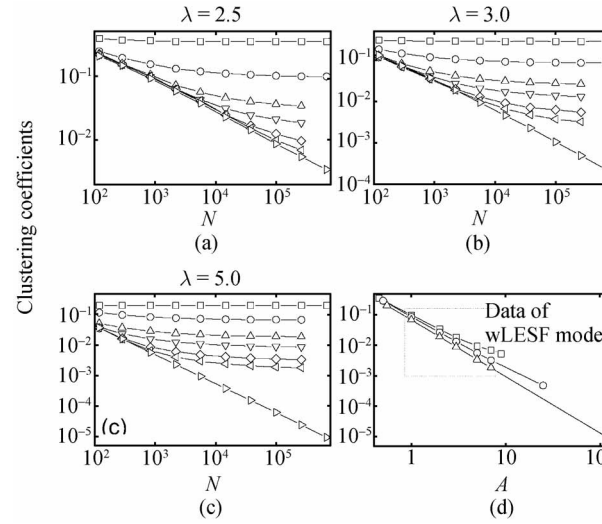

Fig. 3 Clustering coefficients of LESF, WLESF and SFR model. Lines in graphs **(a)**, **(b)** and **(c)** from up to down are the LESF model (*squares*), WLESF model with $A = 1, 2, 3, 5, 7$, and SFR model (*right toward triangles*). **(d)** clustering coefficients C versus the cutoff parameter A in WLESF model, in log-log scale, for $N = 260\,000$ (the last data of WLESF model in **(a)**, **(b)** and **(c)**) and $\lambda = 2.5, 3.0, 5.0$ for squares, circles and triangles respectively; the first and last data of each line are that of LESF model and SFR model respectively, the values of A for these points are adjusted to fit the curve.

To investigate the cascading breakdowns on networks, we employ the sandpile dynamics as follows: (i) At each time step, a grain is added at a randomly chosen node i. (ii) If the height at node i reaches or exceeds a prescribed threshold $z_i = k_i$, the degree of node i; then it becomes unstable and the grains topple to its adjacent nodes: $h_i = h_i - k_i$; and for each neighbor j: $h_j = h_j + 1$; during the transfer, there is a small fraction f of grains being lost, which plays the role of sinks without which the system becomes overloaded in the end. (iii) If this toppling causes any of the adjacent nodes to become unstable, subsequent topplings follow on those nodes in parallel until there is no unstable node left, forming an avalanche event (the cascadings). (iv) Repeat (i)−(iii).

The main feature of the BTW sandpile model is the emergence of a power law with an exponential cutoff in the avalanche area distribution,

$$p(a) \sim a^{-\tau} \mathrm{e}^{-a/a_{\mathrm{c}}} \tag{3}$$

where a_{c} is the characteristic area, i.e., the number of distinct nodes that toppled in an avalanche event.

The avalanche area exponent for different A of WLESF network is shown in Fig. 4. As A goes larger, avalanche area exponent τ increases, and the curves of avalanche area distribution become sharper in the double-log plot (see inset of Fig. 4), which corresponds to fewer large avalanche events. This transition in τ illuminates that when the network is geographically more loosely connected, it will be harder for large cascading events to occur.

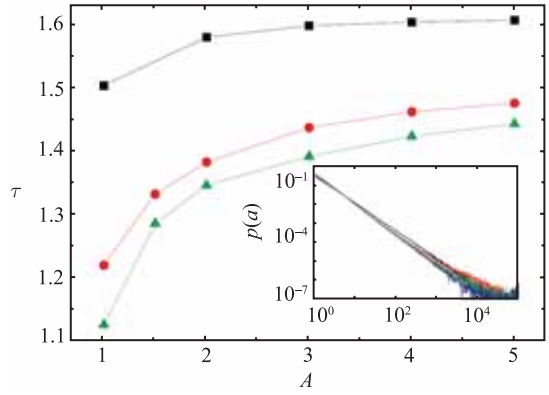

Fig. 4 Avalanche area exponent τ versus the clusterness parameter A, for $\lambda = 3.0$ (*squares*), 5.0 (*circles*) and 10.0 (*triangles*), note that the errorbars in most cases are smaller than the symbol size. The data are fitted by formula 3. *Inset*: avalanche area distribution for $\lambda = 3.0$, from top to bottom are LESF, WLESF $A = 1$, $A = 2$, and SFR networks. The loosing probability is $f = 0.001$, and $m = 4$, $N = 10^5$. Ten network realizations are carried out and for each 10^6 avalanche events are recorded for statistics. The data are log-binned.

The range of an edge is the length of the shortest paths between the nodes it connected in the absence of itself. If an edge's range is l, the shortest cycle it lies on is of length $l+1$. Thus the distribution of range in a network sketches the distribution of shortest cycles. The inset of Fig. 5 shows that when the spatial constraint is slighter, as A goes larger, the range distribution drifts to larger ranges. It means that networks with loose spatial connections have fewer small order cycles but more higher order cycles. If there are many small order cycles, the toppling grains are more likely to meet, and the nodes with fewer grains, i.e., fewer than $z-1$, especially those with $z-2$ or $z-3$ grains, could also reach the toppling threshold z and topple. For example, let $ABCD$ be a quadrangle, and A, B and D are all in their critical height $z_A - 1$, $z_B - 1$ and $z_D - 1$, respectively; if A topples, then B and D will also topple cascadingly, thus C will receive 2 grains. So even if C has less grains than its critical height $z_C - 1$, it could also topple. Larger order cycles contribute less to this effect. The main frame of Fig. 5 shows the fraction of nodes toppled in avalanches that have precisely $z-1$ grains. As the network is less geographically constrained and has fewer small order cycles, the fraction of toppling nodes with $z-1$ grains increases, substantiating our reasoning. This effect contributes to the large avalanche events of the densely connected networks and explains the decrease of avalanche area exponent τ as the network is more geographically constrained. Since many real networks that carry some kinds of loads-e.g., power, traffic, data packets–are imbedded in the $2D$ global surface and highly clustered, our results indicate that they will be at higher risk to suffer breakdowns when there are node failures.

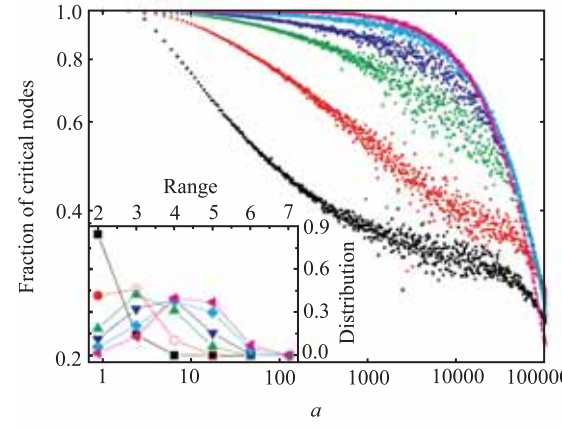

Fig. 5 Fraction of nodes that toppled after receiving only one grain in an avalanche event versus avalanche area. From bottom to top is LESF (*squares*), WLESF $A = 1$ (*circles*), $A = 2$ (*up triangles*), $A = 3$ (*down triangles*), $A = 5$ (*diamonds*), and SFR network (*left triangles*). Each has 10^6 avalanche records on one network for statistics. $\lambda = 3$, $m = 4$, $N = 10^5$. The loosing probability is $f = 0.001$. Inset: range distribution of the same networks; same symbols represent same networks as that in the main frame.

Synchronization is important to many network functions. Now we investigate how the geographical constrains affect the synchronizability of the network. To be concrete, we consider the following general class of coupled-map networks:

$$\boldsymbol{x}_{m+1}^{i} = \boldsymbol{f}(\boldsymbol{x}_{m}^{i}) - \varepsilon \sum_{j} G_{ij} \boldsymbol{H}[\boldsymbol{f}(\boldsymbol{x}_{m}^{j})] \tag{4}$$

where $\boldsymbol{x}_{m+1} = \boldsymbol{f}(\boldsymbol{x}_m)$ is a d-dimensional map, ε is a global coupling parameter, $\boldsymbol{G}$ is the Laplacian matrix, and $\boldsymbol{H}$ is a coupling function. For convenience we choose $G_{ij} = -A_{ij}/k_i$ for $j \neq i$ and $G_{ii} = 1$, where k_i is the degree of node i and A_{ij} is an element of the adjacent matrix $\boldsymbol{A}$ of the network. The eigenvalues of the coupling matrix G are real and nonnegative and can be sorted as $0 = \lambda_1 \leqslant \lambda_2 \leqslant \cdots \leqslant \lambda_N$. Since the rows of the coupling matrix $\boldsymbol{G}$ have zero sum, Eq. (4) permits an exact synchronized solution: $\boldsymbol{x}_m^1 = \boldsymbol{x}_m^2 = \cdots = \boldsymbol{x}_m^N = \boldsymbol{s}_m$, where $\boldsymbol{s}_{m+1} = \boldsymbol{f}(\boldsymbol{s}_m)$. To gain insight, we set $\boldsymbol{f}(\boldsymbol{x})$ to be the one-dimensional logistic

map $f(x) = 1 - ax^2$ ($0 < a \leqslant 2$) and choose $\boldsymbol{H}(\boldsymbol{x}) = x$.

To characterize synchronization, we define synchronization error $\sigma = \langle |x_m^i - \langle x_m^i \rangle| \rangle$, where $\langle \cdot \rangle$ means average over all nodes. It is observed that when the coupling strength ε is greater than a critical value ε_c, $\sigma < 10^{-10}$, i.e., all the oscillators move identically and the system is synchronized. Figure 6 shows the dependence of critical coupling strength ε_c and the synchronization error on the clustering control parameter A. One can see that as A goes larger, both ε_c and σ decreases, indicates a higher synchronizability. That is, when nodes enlarge their circular connecting regions, the network is more synchronizable. The reason of this is that when A is large, a node can connect to a node faraway, thus the network is less locally constrained. This leads to a smaller network distance, as Fig. 7 (a) shows, which means the nodes in the network communicates better, resulting in a better synchronizability. Another factor is that as A increase, the network is more homogeneous in the sense that the maximum load, defined by the number of shortest pathes passing through a node, decreases [Fig. 7 (b)]. Thus the information communication is less jammed and makes for a better synchronizability.

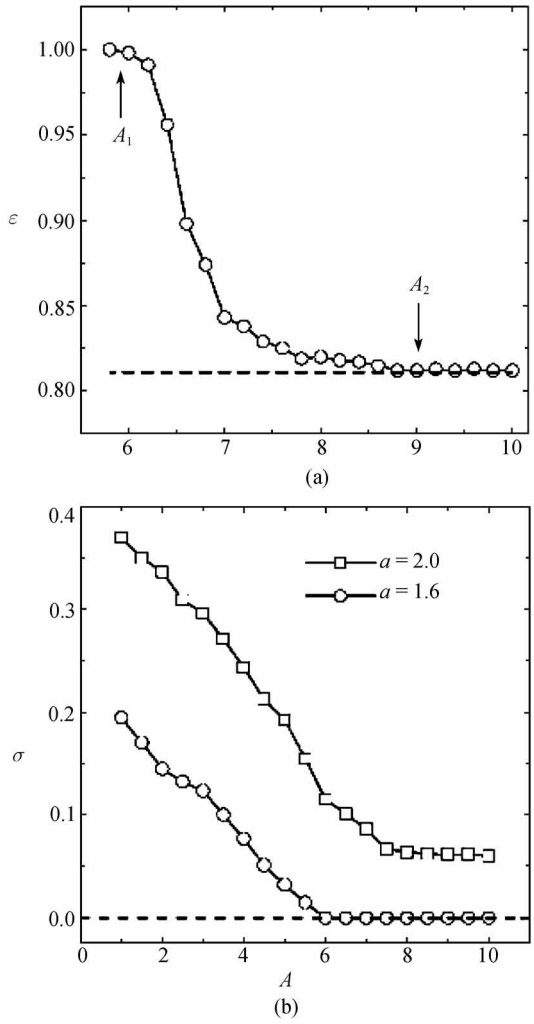

Fig. 6 **(a)** The critical strength parameter ε versus A at $a = 1.60$. **(b)** The synchronization error σ versus A.

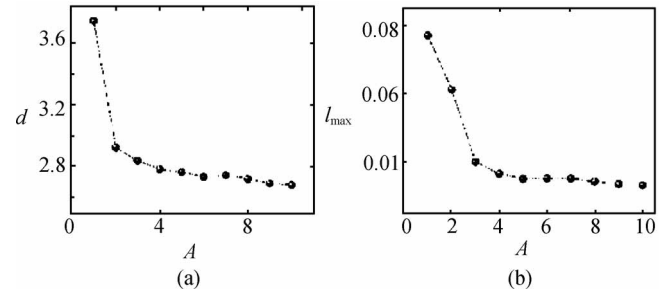

Fig. 7 **(a)** The average network distance versus A. **(b)** The maximum normalized load versus A.

Synchronization on random networks, i.e., each pair of nodes has a probability p to be connected, has been widely studied. Most results concentrates on numerical simulations, recently, using the master stability analysis and the eigenvalue analysis, we provided a theory predicting the synchronization region of the random network for a given dynamical parameter of the system [26].

The coupled system (4) is synchronizable only if the effective coupling strength $K = \varepsilon\lambda_i$ ($i > 1$) falls into a certain interval $(K_1,\ K_2)$, or $K_1 < \varepsilon\lambda_2 \leqslant \cdots \leqslant \varepsilon\lambda_N < K_2$, where K_1 and K_2 depends on the dynamics of a single oscillator only [33]. For 1-D dynamical systems with Lyapunov exponent μ and linear coupling, $K_1 = 1 - \mathrm{e}^{-\mu}$ and $K_2 = 1 + \mathrm{e}^{-\mu}$. The network is synchronizable if $K_1 < \varepsilon\lambda_2$ and $\varepsilon\lambda_N < K_2$. Via eigenvalue analysis, we obtained that

$$\lambda_2 \approx 1 - 2\sqrt{(1-p)/(Np)}$$
$$\lambda_2 \approx 1 + 2\sqrt{(1-p)/(Np)}$$

Therefore, the synchronization condition is

$$\frac{1 - \mathrm{e}^{-\mu}}{1 - 2\sqrt{(1-p)/(Np)}} < \varepsilon < \frac{1 + \mathrm{e}^{-\mu}}{1 + 2\sqrt{(1-p)/(Np)}} \quad (5)$$

[Since in most relevant cases, the upper limit $(1 + \mathrm{e}^{-\mu})(1 + 2\sqrt{(1-p)/(Np)})$ is greater than 1, so in the following, we just discuss the lower limit $(1-\mathrm{e}^{-\mu})(1-2\sqrt{(1-p)/(Np)})$]. Several conclusions are at hand for different limiting cases:

(1) $pC1$, Eq. (5) becomes

$$1 - \mathrm{e}^{-\mu} < \varepsilon \quad (6)$$

which is consistent with the result of globally coupled network (GCN).

(2) Keep p fixed, and let $N \to \infty$, Eq. (5) can also be rewritten as

$$1 - \mathrm{e}^{-\mu} < \varepsilon \tag{7}$$

which implies that in this limit, the behavior of this system would be equivalent to that of a GCN.

(3) Denote $k = Np$, Eq. (5) becomes

$$\frac{1 - \mathrm{e}^{-\mu}}{1 - 2\sqrt{1/k - 1/N}} < \varepsilon \tag{8}$$

If $N \gg k$, then $1/N$ can be neglected, the above equation becomes

$$\frac{1 - \mathrm{e}^{-\mu}}{1 - 2\sqrt{1/k}} < \varepsilon \tag{9}$$

Set $\varepsilon = 1$, the synchronization condition becomes

$$k > K = 4\mathrm{e}^{2\mu} \tag{10}$$

which implies that for ER random networks, one can have chaotic synchronization for arbitrary system size, if the coupling is strong enough, i.e. $\varepsilon = 1$, and if the average degree is larger than some threshold determined by the value of the maximal Lyapunov exponent of the individual dynamics.

Earlier works suggest that small-world and scale-free networks are generally more synchronizable than regular networks. While heterogeneous degree distributions can inhibit synchronization, adding suitable weights to the network elements can enhance their chances to synchronize with each other. In general, given a complex network with a fixed number of nodes, its synchronizability can be improved by increasing the number of links. This is intuitive as a denser linkage makes the network more tightly coupled or, "smaller," thereby facilitating synchronization. A clustered network, which consists of M groups, where nodes within each group are densely connected with probability p_s, but the linkage among the groups is sparse (with probability p_l), however, has a different set of rules that determine the synchronizability [27]. Namely, the synchronizability of a clustered network is determined by the interplay between the inter-connections (links among clusters) and intra-connections (links within clusters) of the network. Strong synchronizability requires that the numbers of the inter-links and intra-links be approximately matched. In this case, increasing the number of links can indeed enhance the synchronizability. However, if the matching is deteriorated, synchronization can be severely suppressed or even totally destroyed.

The synchronization condition of system (4) is $\lambda_2 > (1 - \mathrm{e}^{-\mu})/\varepsilon$. For clustered networks, the normalized eigenvector e_2 corresponded to λ_2, e.g. $Ge_2 = \lambda_2 e_2$, has a special structure that the components of the eigenvector e_2 have approximately the same value within any cluster, while they can vary among clusters. λ_2 can be expressed as $\lambda_2 = e_2^{\mathrm{T}} G e_2$. After lengthy deviation,

$$\lambda_2 \approx \frac{Np_l}{np_s + (N-n)p_l} \tag{11}$$

λ_2 decreases as p_s (or the number of intra-cluster links) increases, which means, for the clustered network, more intra-cluster links, although makes the network smaller, deteriorates the synchronizability of the network.

The synchronization time T-average time required for the system to become synchronized from random initial values-can be used to characterize the ability to synchronize. The less this time, the more synchronizable the system is. But if the system is unstable (unsynchronizable), it can not reach a synchronization state, which means this time equals infinity. Figure 8 shows this synchronization time T vs two control parameters p_l and p_s. This gives the synchronizable region (grey levels in Fig. 8) in the parameter space that the system becomes synchronized within a certain time, and unsynchronizable region (white in Fig. 8) that the time for the system to become synchronized limits to infinity. The lines of the boundaries of the synchronizable and unsynchronizable regions are determined by linear stability analysis (see below). The striking thing Fig. 8 revealed is that for a given p_l (interconnection strength), e.g. $p_l = 0.2$ in Fig. 8 (a), as p_s (intraconnection strength) increases from $p_s = 0.2$, synchronization time T is also increased, and at a certain point (around 0.75 in this case), the system becomes unsynchronizable. So

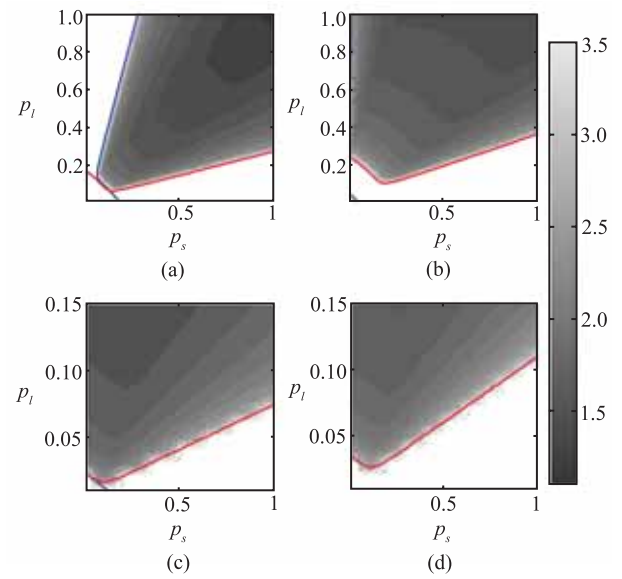

Fig. 8 (*Color online*) Contour plot of the logarithm of the synchronization time T in (p_l, p_s) space for coupled logistic maps with $N = 100$ and $M = 2$ **(a)(b)**, $N = 500$ and $M = 10$ **(c)(d)**, and $\varepsilon = 1$ **(a)(c)**, $\varepsilon = 0.8$ **(b)(d)**. White region means T limits to infinity, which indicates an unsynchronizable region. The boundary lines are determined by theory. Each data point is the result of averaging over 100 network realizations.

it turns out that if the connections within a cluster are too strong, it will destroy the global synchronization. This is reasonable since if the connections within a cluster increase, the cluster itself has stronger ability to synchronize, while relatively, the connections between clusters becomes weaker, and not strong enough to spur different almost synchronized clusters into the globally synchronization state. Thus the whole system is separated into different, almost freely oscillated synchronized clusters.

In conclusion, we shortly reviewed our recent progress on geographical complex networks with respect of statistics, modelling, robustness, and synchronizability. It has been shown that the geographical constrains have important influence on network properties, both topologically and dynamically. Synchronization on random networks and clustered networks is also studied.

Acknowledgements K. Yang thanks the National Hi-Tech Research and Development Program with Grant No. 2006AA093102-08 and the National Basic Research Program of China with Grant No. 2007CB209603 and the Institute of Geology and Geophysics, CAS for their support. L. Yang thanks the 100 Person Project of the Chinese Academy of Sciences, China National Natural Sciences Foundation with Grant No. 10775157 for their support.

References

1. R. Albert and A.-L. Barabási, Rev. Mod. Phys., 2002, 74: 47; M. E. J. Newman, SIAM Rev., 2003, 45: 167
2. S. N. Dorogovtsev and J. F. F. Mendes, Evolution of Networks, Oxford: Oxford University Press, 2003
3. R. Pastor-Satorras and A. Vespignani, Evolution and Structure of the Internet, Cambridge: Cambridge University Press, 2004
4. A. Vázquez, R. Pastor-Satorras, and A. Vespignani, Phys. Rev. E, 2002, 65: 066130
5. C. von Ferber, Yu. Holovatch, and V. Palchykov, Condens. Matter Phys., 2005, 8: 225
6. P. Sen, S. Dasgupta, A. Chatterjee, P. A. Sreeram, G. Mukherjee, and S. S. Manna, Phys. Rev. E, 2003, 67: 036106
7. W. Li and X. Cai, Phys. Rev. E, 2003, 69: 046106
8. R. Guimerà, S. Mossa, A. Turtschi, and L. A. N. Amaral, Proc. Natl. Acad. Sci. USA, 2005, 102: 7794
9. L. Dall'Asta, A. Barrat, M. Barthelemy, and A. Vespignani, Journal Statistical Mechanics, 2006, P04006
10. B. J. Gluckman, T. I. Netoff, E. J. Neel, W. L. Ditto, M. L. Spano, and S. J. Schiff, Phys. Rev. Lett., 1996, 77: 4098
11. A. Barrat, M. Barthélemy, R. Pastor-Satorras, and A. Vespignani, Proc. Natl. Acad. Sci. USA, 2004, 101: 3747
12. A. F. Rozenfeld, R. Cohen, D. ben-Avraham, and S. Havlin, Phys. Rev. Lett., 2002, 89: 218701
13. D. ben-Avraham, A. F. Rozenfeld, R. Cohen, and S. Havlin, Physica A, 2003, 330: 107
14. C. P. Warren, L. M. Sander, and I. M. Sokolov, Phys. Rev. E, 2002,66: 056105
15. P. Sen and S. S. Manna, Phys. Rev. E, 2003, 68: 26104
16. R. Xulvi-Brunet and I. M. Sokolov, Phys. Rev. E, 2002, 66: 026118
17. J. Dall and M. Christensen, Phys. Rev. E, 2002, 66: 016121
18. G. Nemeth and G. Vattay, Phys. Rev. E, 2003, 67: 036110
19. C. Herrmann, M. Barthélemy, and P. Provero, Phys. Rev. E, 2003, 68: 26128
20. W. Zhao, H. He, Z. Lin, and K. Yang, Acta Phys. Sin., 2006, 55: 3906
21. K. Yang, L. Huang, and L. Yang, Phys. Rev. E, 2004, 70: 015102(R)
22. L. Huang, L. Yang, and K. Yang, Europhys. Lett., 2005, 72: 144
23. L. Huang, K. Yang, and L. Yang, Phys. Rev. E, 2007, 75: 036101
24. L. Huang, L. Yang, and K. Yang, Phys. Rev. E, 2006, 73: 036102
25. Z. Lin, L. Yang, and K. Yang, Chin. Phys. Lett., 2005, 22: 3214
26. B. Gong, L. Yang, and K. Yang, Phys. Rev. E, 2005, 72: 037101
27. L. Huang, K. Park, Y.-C. Lai, L. Yang, and K. Yang, Phys. Rev. Lett., 2006, 97: 164101
28. R. Cohen, K. Erez, D. ben-Avraham, and S. Havlin, Phys. Rev. Lett., 2001, 86: 3682
29. P. Holme, B. J. Kim, C. N. Yoon, and S. K. Han, Phys. Rev. E, 2002, 65: 056109
30. D. S. Callaway, M. E. J. Newman, S. H. Strogatz, and D. J. Watts, Phys. Rev. Lett., 2000, 85: 5468
31. R. Cohen, K. Erez, D. ben-Avraham, and S. Havlin, Phys. Rev. Lett., 2000, 85: 4626
32. D. S. Callaway, M. E. J. Newman, S. H. Strogatz, and D. J. Watts, Phys. Rev. Lett., 2000, 85: 5468
33. L. M. Pecora and T. L. Carroll, Phys. Rev. Lett., 1998, 80: 2109